Separation Science and Technology
Publication details, including instructions for authors and subscription information:
http://www.informaworld.com/smpp/title~content=t713708471

Bacterial Community Structure on Membrane Surface and Characteristics of Strains Isolated from Membrane Surface in Submerged Membrane Bioreactor

Piao Jinhua[a]; Kensuke Fukushi[a]; Kazuo Yamamoto[a]
[a] Environmental Science Center, The University of Tokyo, Bunkyo-ku, Tokyo, Japan

To cite this Article Jinhua, Piao , Fukushi, Kensuke and Yamamoto, Kazuo(2006) 'Bacterial Community Structure on Membrane Surface and Characteristics of Strains Isolated from Membrane Surface in Submerged Membrane Bioreactor', Separation Science and Technology, 41: 7, 1527 — 1549
To link to this Article: DOI: 10.1080/01496390600683571
URL: http://dx.doi.org/10.1080/01496390600683571

Separation Science and Technology, 41: 1527–1549, 2006

ISSN 0149-6395 print/1520-5754 online
DOI: 10.1080/01496390600683571

Bacterial Community Structure on Membrane Surface and Characteristics of Strains Isolated from Membrane Surface in Submerged Membrane Bioreactor

Piao Jinhua, Kensuke Fukushi, and Kazuo Yamamoto
Environmental Science Center, The University of Tokyo,
Bunkyo-ku, Tokyo, Japan

Abstract: In order to investigate the bacterial community structure and the characteristics of bacteria on the membrane surface, a submerged membrane bioreactor treating municipal wastewater was continuously operated under two different conditions. Bacterial community structures were examined by PCR-denaturing gradient gel electrophoresis and PCR cloning of 16S rRNA genes. Bacterial strains isolated from membrane surface were identified and their growth curve, EPS concentration and hydrophobicity were measured. The structures of bacterial communities in the suspended solids and on the membrane surface were obviously different, and *γ-Proteobacteria* more selectively adhere and grow on the membrane surface than other microorganisms. Most of the membrane isolates grew slowly as compared with the strains isolated from the suspended solids. Also, the membrane isolates were higher cell surface hydrophobicities, higher EPS concentrations, and higher ratios of protein to carbohydrate within the EPSs than the isolates from suspended solids.

Keywords: Submerged membrane bioreactor, bacterial community structure, *γ-Proteobacteria*, characteristics of isolate

INTRODUCTION

A membrane bioreactor (MBR) system, a membrane technology combined with biological reactors for the treatment of wastewaters, is one of the

Received 8 March 2006, Accepted 13 March 2006
Address correspondence to Piao Jinhua, Environmental Science Center, The University of Tokyo, 7-3-1 Hongo, Bunkyo-ku, Tokyo 113-0033, Japan. E-mail: parkjh@env.t.u-tokyo.ac.jp

advanced wastewater treatment processes. The advantages of MBR are a higher biomass concentration of up to 15 g/l permitting a high water product quality and a smaller excess sludge production than in the case of the conventional activated sludge process (1). A submerged MBR system (2), in which a membrane unit is directly immersed in an activated sludge bioreactor, was developed to be more compact, more energy efficient, and much improved in terms of minimized membrane fouling by a low-flux operation.

Although membrane fouling has been improved greatly with the development of submerged MBR, it is still a limiting factor in determining MBR performance, that is higher operating pressures, frequent chemical cleaning, and shortened membrane life. Various methods have been adopted to control membrane fouling: backwashing, jet aeration, operation at lower than a critical or subcritical flux, addition of coagulants, and intermittent permeation, etc. (3–7). However, these physicochemical approaches only can partially solve the problem on a temporary basis.

Biofouling has become a significant concern in an MBR system. Biofouling is more complicated than other membrane fouling phenomena because microorganisms can grow, multiply, and relocate there. Numerous researchers verified that extracellular polymeric substances (EPS) are one of the important foulants in MBR (8–10). These investigations of EPS effects on membrane fouling were carried out using various model bacteria that produce large amount of EPS to accelerate the fouling, but it may lose the complexity inherent in multispecies biofouling. The microbial community of suspended solids in MBR for treating real wastewater has been investigated (11, 12). However, there is a lack of information on what types of bacterium adhere and grow on the membrane and how the multiplication and relocation of bacteria on it affect the progress of membrane fouling.

The objective of this study, therefore, is to investigate the bacterial community structure and the characteristics of bacteria on the membrane surface.

MATERIALS AND METHODS

A pilot-scale MBR for treating municipal wastewater was continuously operated under low- and high-volumetric organic load (VOL) conditions. The low VOL condition reflected a small-scale MBR process similar to a Jokaso system (an onsite domestic wastewater treatment process), and the high VOL condition reflected a large-scale MBR process. Membrane fibers and suspended solids were sampled periodically for bacterial identification. The bacterial community structures were examined by culture-independent, molecular biology-based methods, such as PCR-denaturing gradient gel electrophoresis (PCR-DGGE) and PCR cloning of 16S rRNA genes. For characterizing bacteria adhering on the membrane surface, bacterial strains

isolated from membrane surface were identified and their growth curve, EPS concentration, and hydrophobicity were measured.

Membrane Bioreactor

A pilot-scale submerged MBR (Fig. 1) for treating real municipal wastewater was placed at a municipal wastewater treatment plant located in Tokyo, Japan. Activated-sludge mixed liquor, taken from the return sludge line of the plant, were inoculated within a volume of 150 liters. A microfiltration (MF, Mitsubishi-Rayon Co.) membrane module with an effective surface area of $3\,m^2$ was submerged in the reactor to control hydraulic retention time (HRT). The MF membrane of the hollow-fiber type was made of polyethylene. Its pore size was 0.4 μm. Several small membrane modules with an effective surface area of $0.03\,m^2$ were used for the sampling of membrane fibers instead of the large module mentioned above. Except for the effective surface area, the characteristics of small membrane modules were the same as those of the large module. The flux of small membrane modules was controlled similarly to the large module. Several small membrane modules that were set initially were sampled individually periodically. The change in HRT caused by that sampling was negligibly small.

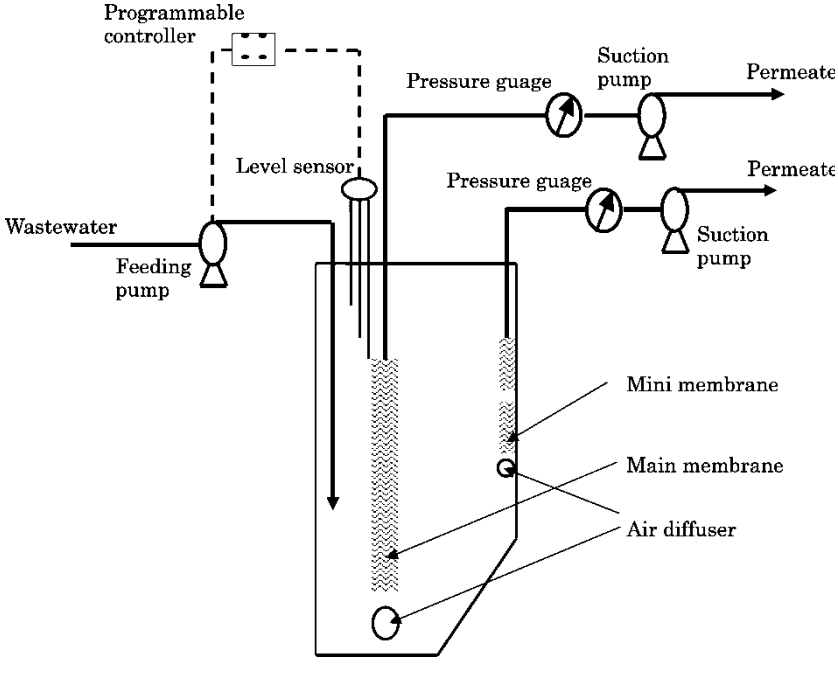

Figure 1. Schematic diagram of suspended MBR.

MBR was continuously operated twice at different HRTs. The first run was operated at an HRT of 1 day, and a flux of 0.05 m/d. After 3 months of the run, MLSS concentration increased from 1.7 g/l to about 4.0 g/l and became stable. Five small membrane modules were sampled periodically during this period. HRT was then changed to 6 h and flux to 0.2 m/d. When MLSS concentration increased to approximately around 7.0 g/l, six small membrane modules were added and periodic sampling was started until the MLSS concentration became stable at 10.3 g/l. During the entire period of the operation, no sludge was wasted from the reactor except for sampling. During the entire period, dissolved oxygen (DO) concentration of the mixed liquor was maintained in the range from 3 to 4.5 mgO_2/l, temperature in the range from 18 to 20°C, and pH in the range from 6.5 to 7.3. The treatment performance was monitored by measuring the total or dissolved organic carbon (TOC or DOC) concentration of the influent and effluent using a TOC-500 (Shimazu) analyzer. MLSS concentration was also measured by the standard method (Japan).

Sampling

In each period, membrane fibers were sampled periodically simultaneously with the sampling of suspended solids. Suspended solids samples of 1 ml were collected from MBR, and centrifuged at 10,000 rpm for 5 min. Obtained pellets were resuspended in 0.8 ml of TE buffer (10 mM Tris-HCl, 1 mM EDTA, pH 8.0) and then centrifuged again. After discarding supernatant, the remaining pellets were kept at −20°C for DNA extraction. Membrane fibers were obtained from small membrane modules and washed by vortex mixing with TE buffer to remove loosely attached bacteria. After washing, the membrane fibers were stored at −20°C for DNA extraction.

DNA Extraction

Genomic DNA was extracted using a FastDNA SPIN kit for soil (Bio 101, Q-BIOgene) following the instructions from the manufacturer. For suspended solids, 0.5 ml of a sample was used. For membrane samples, membrane fibers were sliced into small fragments with a total surface area of approximately 0.001 m^2 and then used for extraction. Extracted DNA was quantified by measuring the UV absorption spectrum.

PCR-DGGE

The variable V3 region of genetic 16S rRNA were amplified from the extracted genomic DNA by PCR using a T3Thermocycler (Biometra) and

primers 357f-GC (5′-CCTACgggAggCAgCAg-3′) and 518r (5′-ATTACCgCggCTgCTgg-3′) (13). The final 50-μl reaction mixture contained 1 × PCR buffer, 0.15 mM $MgCl_2$, 200 μM deoxynucleoside triphosphate, 200 nM of forward and reverse primers, 0.025 U of Taq DNA polymerase (Amplitaq Gol; Perkin-Elmer), and 1 μl of template DNA. The PCR was conducted with the initial denaturation at 95°C for 10 min, followed by 30 cycles of 94°C for 30 s, 53°C for 30 s, 72°C for 30 s and then a final extension at 72°C for 10 min prior to cooling at 4°C.

DGGE was carried out as described by Muyzer (13), using the D-code universal mutation detection system (Bio-Rad Laboratories) and 8% polyacrylamide gels containing denaturant gradients from 35% to 60% for the analysis of 357f-GC plus 518r PCR products. Electrophoresis was performed in 0.5 × Tris-acetate-EDTA (TAE) buffer at a constant voltage of 130 V and a temperature of 60°C. After electrophoresis, the gels were stained with 10,000-fold diluted VistraGreen solution (Amersham-Pharmashia) for 15 min and rinsed with Milli-Q water. Gel images were obtained using a fluorescence image analyzer, FluorImager 595 (Molecular Dynamics).

PCR Cloning and Sequencing

Nearly complete 16S rRNA genes were amplified by PCR as described above except that primers 27f (5′-AgAgTTTgATCMTggCTCAg-3′) and 1492r (5′-TACggYTACCTTgTTACgACTT-3′) (14) were used. PCR products were purified, ligated into the pDrive Cloning vector (QIAGEN), and transformed into competent *Escherichia coli* cells supplied with a QIAGEN PCR Cloning kit (QIAGEN). Blue-white screening was performed according to the manufacturer's instructions. White colonies on Luria-Bertani plates were selected and subjected to PCR using primers SP6 and T7, and inserts were detected by agarose gel electrophoresis with subsequent ethidium bromide staining. The PCR conditions and the composition of the reaction mixtures were the same as those described above, except that a small number of *Escherichia coli* cells picked from a colony with a needle were added instead of DNA. Clones were screened by the PCR-DGGE method.

Prior to sequencing, DNA templates were purified using a Montage SEEQ96 Sequencing Reaction Cleanup kit (Millipore Co.). DNA sequencing was carried out using an ABI Prism BigDye terminator sequencing kit (PE Applied Biosystems) and an ABI 3100 DNA sequencer (PE Applied Biosystems).

Phylogenetic Analysis

Sequences were compared with those in available databases using the BLAST network service on DDBJ (15) to determine their approximate phylogenetic

affiliations. Ribosomal DNA sequences were aligned and analyzed using the ClustalW software package (16). Phylogenetic trees were constructed using the neighbor-joining method (17) in the programs of the phylogeny inference package (PHYLIP).

Isolation and Identification of Bacteria from Membrane and Suspended Solids

Pellets formed after centrifugation of suspended solids at 3500 rpm for 10 min were resuspended in nutrient broth (5.0 g of peptone, 3.0 g of beef extract per liter of distilled water, and final pH of approximately 7.0) and vigorously vortexed. Appropriate dilutions of the bacterial resuspension were plated on nutrient agar, which was composed of (per liter) 5.0 g of peptone, 3.0 g of beef extract, and 15.0 g agar. Membrane fibers were washed in distilled water with vortex mixing prior to their inoculation to the nutrient broth. Bacteria were dislodged from the membrane surface to the nutrient broth by sonication at 80 W for 2 min in an ice-water bath and then the inocula were serially diluted. Appropriate dilutions were spread onto nutrient agar plates. After incubation at 20°C for up to 1 week, plates containing approximately 50 colonies were examined, and up to three representative colonies of each of the different types that appeared were picked. Selected colonies were purified by streaking them onto fresh nutrient agar and used subsequently for DNA extraction. Morphologically similar colonies were screened by PCR-DGGE described above, and their representative isolates and other remaining isolates were identified by the sequencing almost full-length 16S rDNA genes described above. The gram staining and other characteristics (see below) of isolates were examined.

Characterization of Bacterial Isolates

Growth Curve

The bacterial isolates were precultured in a test tube containing nutrient broth at 20°C on a shaker, and bacterial growth was monitored by measuring optical density at 600 nm (OD_{600}) with a spectrophotometer (Hitachi). When OD_{600} was in the range from 0.6 to 0.7, 1.5 ml of a culture was inoculated into a flask containing 150 ml of fresh nutrient broth. Growth curves were based on the OD_{600}.

EPS Extraction and Measurement

The method of Pavoni et al. was used with modifications. Cells were harvested by the centrifugation of 10 ml of culture at 3500 rpm for 5 min at 4°C and

washed with distilled water twice prior to extraction to remove nutrient broth from cells. The pellet obtained was resuspended to 5 ml of distilled water and centrifuged at 15,000 rpm for 10 min at 4°C. The EPS of isolates was obtained by the filtration of supernatants through a cellulose acetate filter with a pore size of 0.2 μm. Cell dry weight in a culture was measured by weighing the residue obtained following filtration through a cellulose acetate filter with a pore size of 0.2 μm, and drying for 2 to 4 hours to a constant weight at 105°C. Total organic carbon (TOC) concentration in EPSs was measured with TOC-500 (Shimazu). For the quantitative analysis of carbohydrate in EPSs, the phenol-sulfuric acid method was used with glucose as a standard (18). Total protein concentration in EPSs was quantified by the bicinchoninic acid (BCA) method according to the manufacturer's instructions.

Cell Surface Hydrophobicity

The surface hydrophobicity of isolates was examined by the method of Rosenberg et al. (19) with some modifications. Cells were harvested by the centrifugation of a 1.4-ml culture at 3500 rpm for 5 min at 4°C. The resulting pellet was washed and resuspended in 1 × phosphate-buffered saline (PBS, pH of 7.2) and then OD_{600} was determined. The suspension was mixed for 15 s with 0.35 ml n-hexadecane using a vortex mixer and the mixture was allowed to stand for 15 min, after which the absorbance of the water phase was measured at 660 nm (OD_{660}). Hydrophobicity was calculated as follows.

$$hydrophobicity = \frac{OD_{600} - OD_{660}}{OD_{600}}$$

RESULTS

Due to the nature of actual municipal wastewater, the influent TOC concentration fluctuated weekly and seasonally; therefore, the average TOC concentration was used to calculate volumetric organic load (VOL). The average TOC concentration of the municipal wastewater during the entire experimental period was 81.8 mgTOC/l and the VOL of the first run was 0.082 kgTOC/m^3/d. This operating condition was designated as a low-VOL condition in this study. Under this condition, effluent DOC concentration was maintained at about 5 mg/l. Five membrane samples (ML7, ML13, ML29, ML47, and ML68, sampled on days 7, 13, 29, 47, and 68, respectively) obtained simultaneously with suspended solid samples were obtained during this period, and the corresponding TMP and the MLSS concentrations are shown in Table 1. Transmembrane pressure (TMP) increased from 5 to 12 kPa during 3 months of operation under the low-VOL condition. TMP is an important factor for evaluating the performance of a submerged MBR because it is directly related to membrane fouling. TMP changes in this case indicated that membrane fouling was not severe under the low-VOL condition.

Table 1. TMP of membrane samples and MLSS concentration of suspended solids samples. In the name of samples, M and S represent the membrane and suspended solids, respectively; L and H represent the low volumetric organic loading (VOL) and high VOL, respectively; the following number show the operating days. For example, ML47 and SL47 are the samples of the membrane and suspended solids, respectively, obtained simultaneously on 47 days under the low VOL operating condition

Sample		TMP, kPa	MLSS, g/l
Low VOL			
ML7	SL7	8	2.17
ML13	SL13	8	2.04
ML29	SL29	8	2.20
ML47	SL47	10	3.40
ML68	SL68	12	3.64
High VOL			
MH12	SH12	10	7.80
MH22	SH22	12	8.30
MH32	SH32	16	10.1
MH42	SH42	40	10.5
MH52	SH52	80	10.3

At an HRT of 6 h and a flux of 0.2 m/d, the VOL was 0.327 kgTOC/m^3/d. This operating condition was designated as a high-VOL condition. The DOC concentration of effluent was less than 12 mg/l during this period. Five membrane samples (see Table 1, MH12, MH22, MH32, MH42, and MH52, sampled on days 12, 22, 32, 42, and 52, respectively) collected simultaneously with suspended solid samples (SH12, SH22, SH32, SH42, and SH52 in the Table 1) were obtained under the high VOL condition. TMP increased to 40 kPa after operating for 42 days under the high-VOL condition, indicating that severe fouling occurred during this period. The dynamic variation on the membrane surface with the progress of fouling was investigated by a scanning electron microscopy (SEM). Membrane pores on a virgin hollow fiber MF membrane utilized in this study were clearly observed on a SEM photomicrograph (Fig. 2(a)). Comparing the SEM photomicrographs of the virgin membrane with those of membranes that insignificantly fouled, namely MH12, MH22, and MH32 with TMPs of 10, 12, and 16 kPa, respectively, showed surfaces with similar structures and the shape of cells could be resolved (Fig. 2(b)–(d)). In contrast, the significantly fouled membrane MH42 with a TMP of 40 kPa showed a surface that was less rough than those of insignificantly fouled membranes and partially covered with a flat cake layer, indicating that the accumulation of microorganisms is not a factor that directly cause a significant increase in TMP but it could lead to the development of a cake layer that cause the significant fouling.

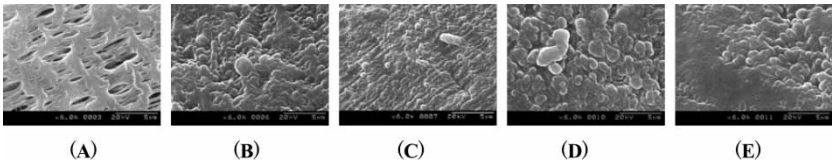

Figure 2. SEM photomicrographs show the surface of virgin hollow fiber MF membrane utilized in this study (A) and the of used membrane samples: (B), the membrane sample MH12 with the TMP of 10 kPa; (C), the membrane sample MH22 with the TMP of 12 kPa; (C), the membrane sample MH32 with the TMP of 16 kPa; (E), the membrane sample MH42 with the TMP of 40. Original magnification, $\times 6000$; bar, 5 μm.

Structure of Bacterial Community on Membrane Surface under Different Operating Conditions

Low-VOL Condition

In order to compare bacterial community structures between the membrane samples and suspended solids samples, and also to investigate fluctuations in the community structure with the progress of fouling, DGGE using partial 16S rDNA fragments was applied. Under the low-VOL condition, DGGE profiles (data not shown) of the membrane samples were completely different from those of the suspended solid samples even between those simultaneously collected membrane and suspended solid samples. Individual bands corresponding to individual membrane samples, however, did not show any trends of increasing or decreasing signal intensity with TMP increase.

To characterize the compositions of bacterial communities, almost full-length 16S rDNA sequences obtained from the membrane samples and suspended solid samples were phylogenitically analyzed by PCR cloning and sequencing assay. Clone libraries of the membrane samples ML7 and ML47 obtained on days 7 and 47, respectively, as well as the suspended solids sample SL47 under the low-VOL condition were generated (Table 2). Most clones in each clone library were assigned to *Proteobacteria*. One sequence (7 clones) in the ML7, one clone in the ML47, and one sequence (16 clones) in the SL47, could not be assigned to any known bacterial divisions. However, these were assigned to be candidate divisions of *Bacteroidetes* (see clone ML7-4 in Fig. 7), *Xanthomonadaceae* of *γ-Proteobacteria* (see clone ML47-5 in Fig. 5), and *α-Proteobacteria* (see clone SL47-15 in Fig. 8), respectively in the phylogenetic analysis. In the suspended solids clone library SL47, clones belonging to *α-Proteobacteria* were the most abundant whereas in the membrane clone libraries ML7 and ML47, clones belonging to *γ-Proteobacteria* were the most abundant. More interestingly, 32.2% and 23.8% of all clones in the clone libraries of ML7 and ML47, respectively, were assigned to the *Xanthomonadaceae* family of *γ-Proteobacteria*,

Table 2. Distribution of clone and isolate sequences in phylogenetic groups

Phylogenetic group	Relative clone abundance (%) in:				Number of colonies from:	
	ML7 (33)[a]	ML47 (21)	SL47 (52)	MH12 (130)	MH12 (20)[b]	SH12 (23)
α-Proteobacteria	3.0	4.8	38.5	10.0	3	2
β-Proteobacteria	21.2	4.8	13.5	20.8	4	2
γ-Proteobacteria	51.5	57.1	1.9	50.0	4	15
δ-Proteobacteria	0.0	0.0	0.0	4.6	0	0
Firmicutes	0.0	19.0	1.9	2.3	3	4
Actinobacteria	0.0	4.8	5.8	4.6	1	0
Bacteroidetes	0.0	4.8	7.7	6.2	0	0
Spirochaetales	0.0	0.0	0.0	1.5	0	0
Flavobacteria	0.0	0.0	0.0	0.0	5	0
Unclassified groups	21.2	4.8	30.8	0.0	0	0

[a]A number in parentheses indicates the total number of clones obtained from each samples.

[b]A number in parentheses indicates the total number of colonies obtained from the MH12 and SH12, respectively.

with more than 96% similarity. In contrast, only 1 clone (see clone SL47-5 in Fig. 5) in SL47 showed 95 % similarity with *Thermomonas brevis*. Although a few highly similar clones (>98% identical) were detected both in ML47 and SL47 [see sequences ML47-16 (2 clones) and SL47-20 (3 clones), sequences ML47-17 (1 clone) and SL47-51 (1 clone) in Fig. 8; see sequences ML47-3 (1 clone) and SL47-31 (2 clones) in Fig. 6; see sequences ML47-13 (1 clone) and SL47-5 (1 clone) in Fig. 5], there were substantial differences between these two bacterial communities.

High VOL Condition

Similar to the results obtained under the low-VOL condition, differences in the DGGE banding patterns between membrane samples and suspended solid samples were observed under the high-VOL condition (Fig. 3). Interestingly, the DGGE banding profiles for the membrane samples showed major changes in the community structure with the progress of fouling. Bands A, B, C, D, and E were predominant for the membrane samples MH12, MH22, and MH32, which were not significantly fouled membranes, and were absent or present only as faint bands for the membrane samples MH42 and MH52, which were completely fouled membranes. In contrast, bands F, G, and I, which were present as faint bands (e.g., bands F and G) or absent (e.g., band I) for MH12 showed a trend of increasing signal intensity with the progress of fouling.

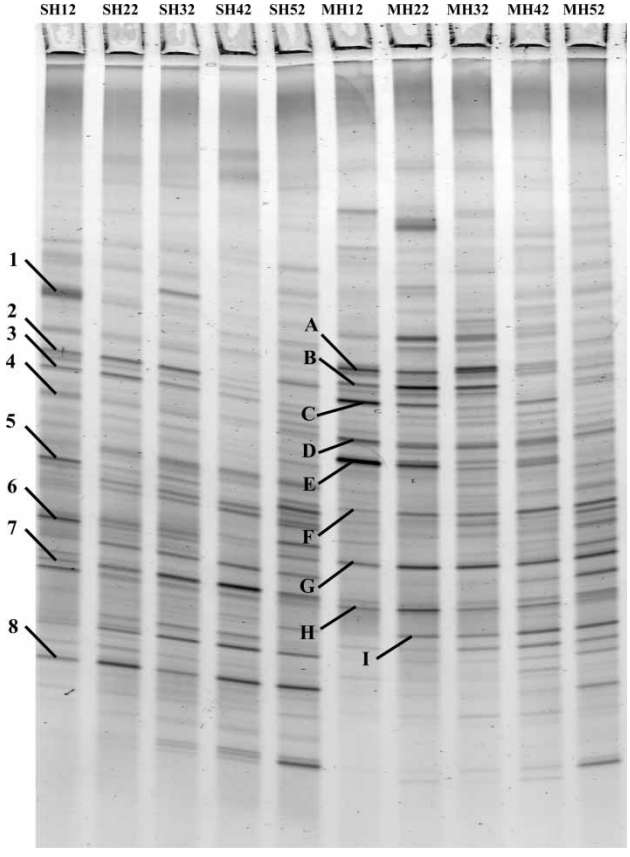

Figure 3. DGGE profiles of the partial 16S rDNA fragments generated by membrane samples and suspended solids samples that obtained from high VOL operating condition. Lanes are designated by name of the samples. SH12 to SH52, DGGE profiles of suspended solids; MH12 to MH52, DGGE profiles of membrane samples. Details of each sample are shown in Table 1. Predominant bands in the membrane samples are expressed as A-I; predominant bands in the suspended samples are expressed as 1–8.

Clones of nearly full-length 16S rDNA were obtained from MH12 and SH12 by PCR cloning, and the clone library of MH12 was constructed (Table 2) by DGGE screening followed by sequencing. Similar to the results obtained under the low-VOL condition, 50% of 130 clones in the MH12 clone library were assigned to *γ-Proteobacteria*, indicating that bacteria belonging to *γ-Proteobacteria* were predominant on the membrane surface. However, except for one sequence (2 clones, see clone MH12-36 in Fig. 5) assigned to *Xanthomonas axonopodis* with a similarity of 99%, most of the clones belonging to *γ-Proteobacteria* were regarded as unidentified

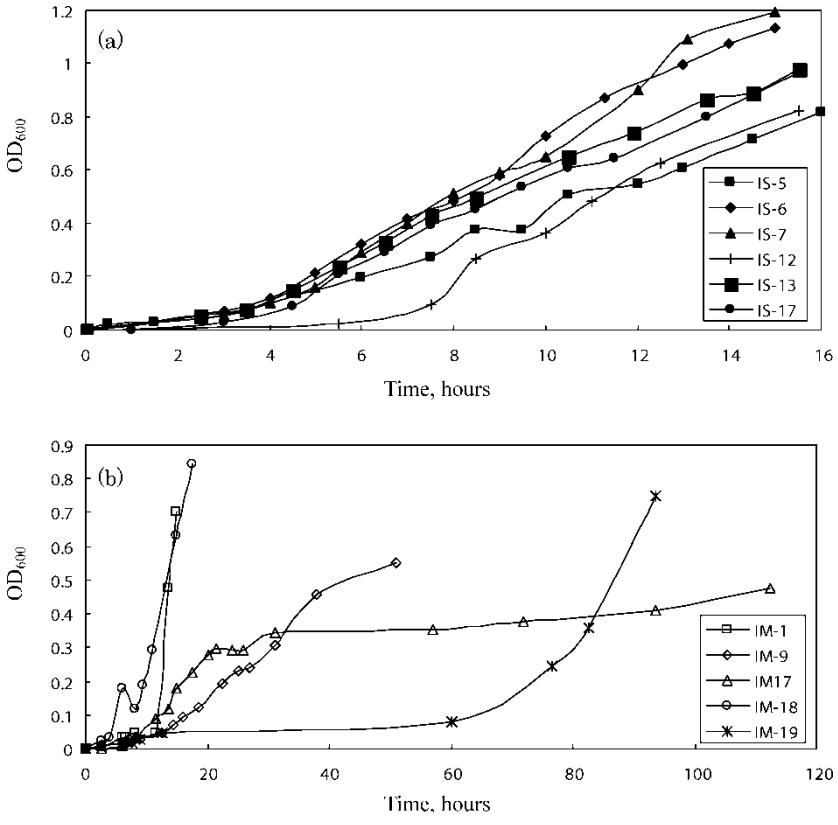

Figure 4. Growth curves of suspended solids isolates (a) and membrane isolates (b).

γ-Proteobacteria because of their low similarities (<93%) with related sequences in database. The second most abundant clones (20.8% of all clones) were assigned to *β-Proteobacteria*, and most of them belonged to the *Burkholderiales* subdivision of *β-Proteobacteria*. Bacterial divisions of *δ-Proteobacteria* and *Spirochaetales* that did not appear under the low-VOL condition were found on the membrane surface under the high-VOL condition.

To determine the clones corresponding to predominant bands A to I and bands 1 to 8 in the DGGE profiles (Fig. 2), among clones obtained from MH12 and SH12, at least two clones that corresponded to those distinct bands on DGGE gel were selected and sequenced. As shown in Table 3, all of the predominant bands for the membrane sample, except bands A and B assigned to *β-Proteobacteria*, were related to *γ-Proteobacteria*. In contrast, the clones corresponding to the bands for the suspended solid sample belonged to a relatively broad phylogenetic distribution, including *Bacteroidets*, *Firmicutes*, *Actinobacteria*, and *Proteobacteria*. A clone that corresponded to band I was not found when comparing the clones generated from MH12 with those

Table 3. Identification of DGGE bands from Fig. 2

Band no.	Clone no.	Sequence length (bases)	Phylogenetic relationship		
			Most closely related sequence (Accession no.)	Bacterial division	% Identity
A	MH12-27	1498	Uncultured Aquabacterium sp. (AF523042)	*β-Proteobacteria*	95
B	MH12-86	1403	*Imtechium assamiensis* (AY544767)	*β-Proteobacteria*	96
C	MH12-104	1486	Uncultured bacterium (AY212663)	*γ-Proteobacteria*	96
D	MH12-3	1572	Uncultured bacterium (AY212663)	*γ-Proteobacteria*	95
E	MH12-122	1490	Uncultured bacterium (AY212663)	*γ-Proteobacteria*	96
F	MH12-58	1592	Uncultured bacterium (AY218736)	*γ-Proteobacteria*	84
G	MH12-7	1572	*Moraxella lacunata* (AF005170)	*γ-Proteobacteria*	91
H	MH12-37	1004	*Enhydrobacter aerosaccus* (AJ550856)	*γ-Proteobacteria*	90
1	SH12-15	1411	Uncultured Bacteroidetes bacterium (AY211071)	*Bacteroidets*	97
2	SH12-53	1438	Unidentified rumen bacterium RC6 (AF001699)	*Firmicutes*	87
3	SH12-40	1494	Comamonadaceae bacterium MPsc (AY651926)	*β-Proteobacteria*	96
4	SH12-96	1492	Comamonadaceae bacterium MPsc (AY651926)	*β-Proteobacteria*	96
5	SH12-93	1511	*Frateuria aurantia* (AB091199)	*γ-Proteobacteria*	91
6	SH12-33	1449	*Mesorhizobium ciceri* (AY206686)	*α-Proteobacteria*	96
7	SH12-92	1446	Gamma proteobacterium (AJ630298)	*γ-Proteobacteria*	96
8	SH12-17	1493	Uncultured bacterium ARFS-6 (AJ277690)	*Actinobacteria*	97

from sample MH22 on the DGGE gel, indicating that microorganisms corresponding to band I did not exist in sample MH12. The phylogenetic positions of each band are shown in Figs. 5 to 8; clones corresponding to bands C, D, and E belonged to unclassified group of *γ-Proteobacteria*

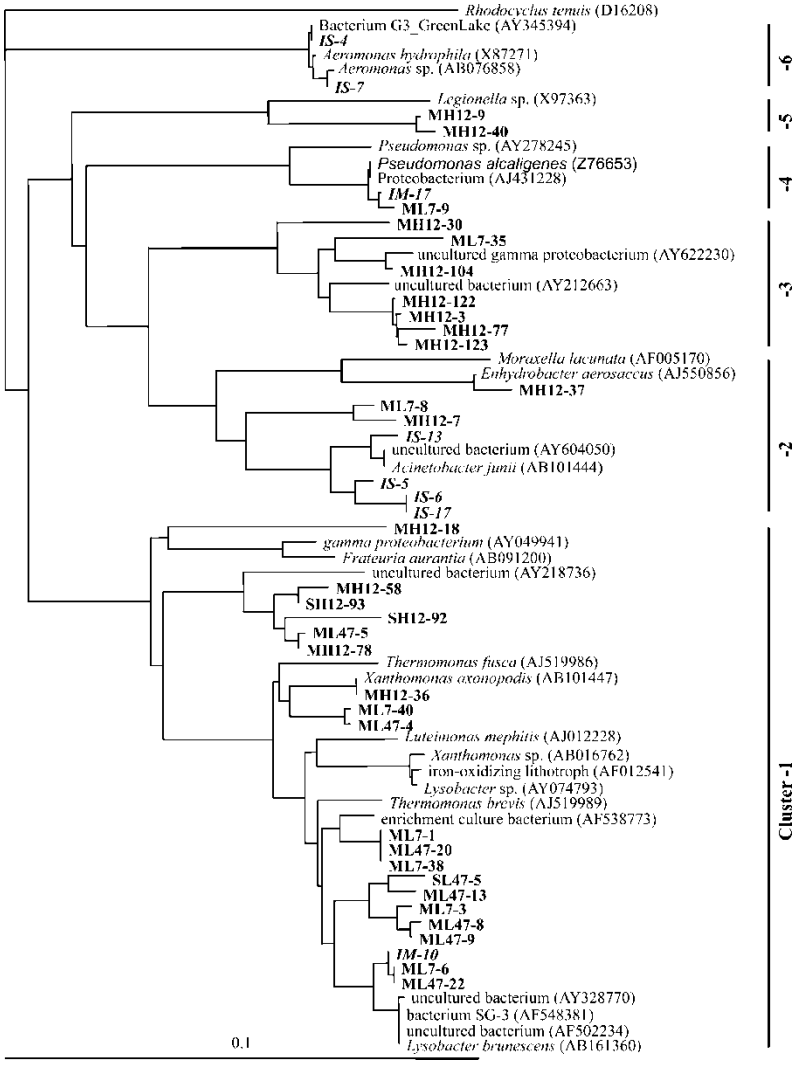

Figure 5. Phylogenetic tree of the *γ-Proteobacteria* clones and isolates. For the clones, the names are in bold and designated by the sample name followed by the number. Isolates are in bold and italics. Accession numbers appear in parentheses for all reference sequences. Cluster 1 to 6 represent *Xanthomonadaceae*, *Moraxellaceae*, unclassified group, *Pseudomonadaceae* and *Aeromonadaceae* family or group of the *γ-Proteobacteria*, respectively. The scale bar indicates 0.1 changes per nucleotide.

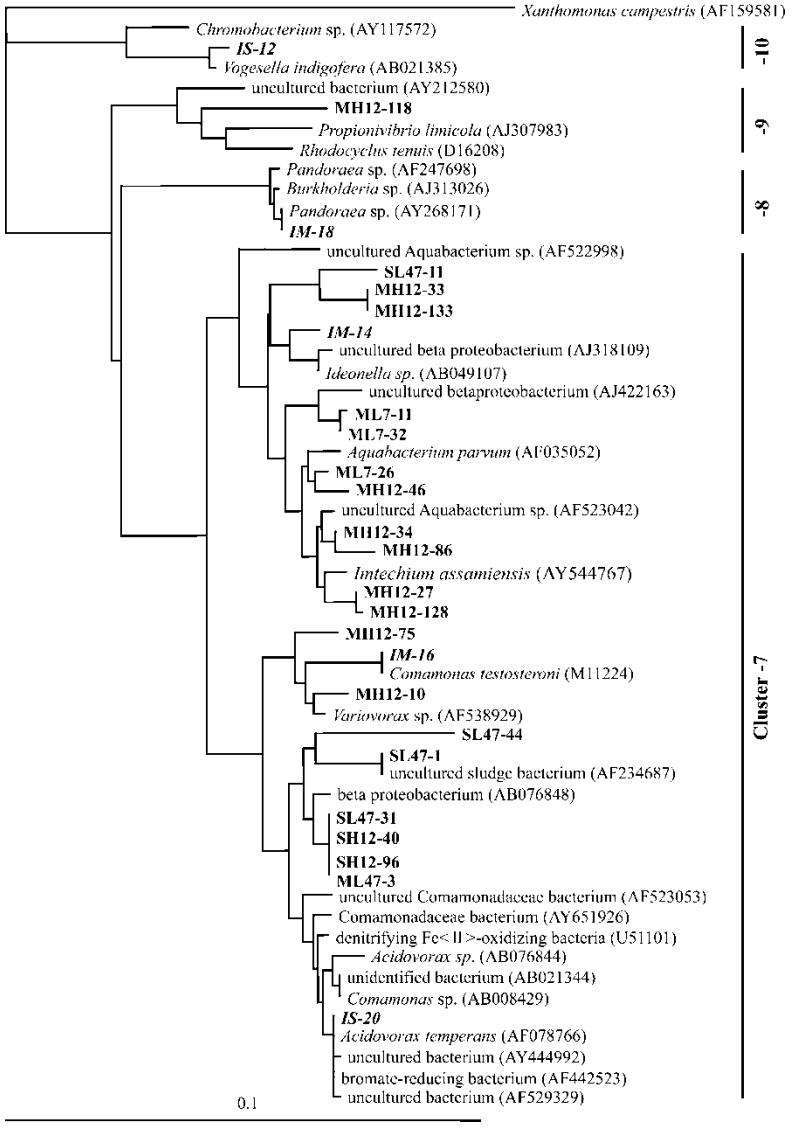

Figure 6. Phylogenetic tree of the *β-Proteobacteria* clones and isolates. Cluster 7 to 10 represent *Comamonadaceae*, *Burkholderiaceae*, *Rhodocyclaceae* and *Neisseriaceae* family or group of the *β-Proteobacteria*, respectively. Other notation is as described for Fig. 5.

(see cluster 3 in Fig. 5), clones corresponding to bands F belonged to the *Xanthomonadaceae* (see clone MH12-58 in cluster-1, in Fig. 5), and clones matching bands G and H belonged to the *Moraxellaceae* family of *γ-Proteobacteria*. Clones MH12-58 and SH12-93, corresponding to two putatively the

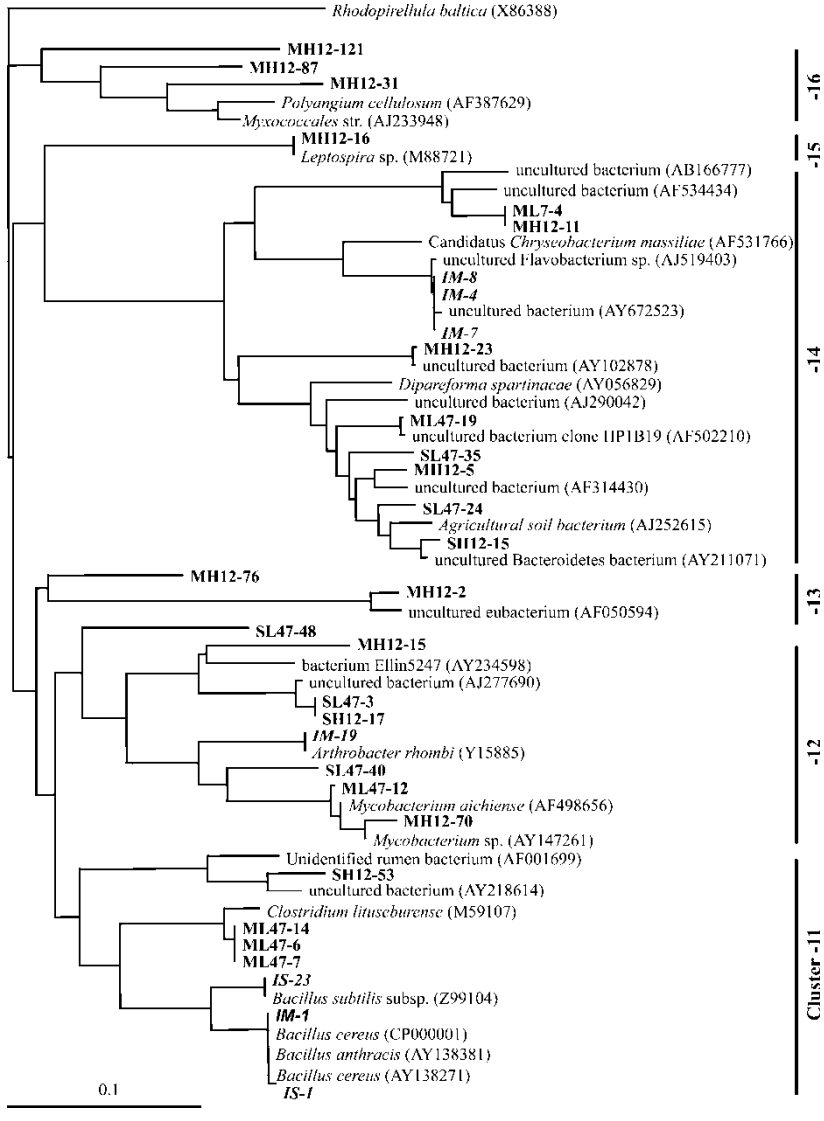

Figure 7. Phylogenetic tree of clones and isolates those are not associated with the *Proteobacteria* of the α, β, and γ subcluss. Cluster 11 to 16 represent *Firmicutes*, *Actinobacteria*, unclassified phylum, *Bacteroidetes*, *Spirochaetes* and δ-*Proteobacteria*, respectively. Other notation is as described for Fig. 5.

same vertical gel position bands F and 5, respectively, had a high similarity (96%), indicating that these two bands represent the same organism. B and 5 was predominant only during the initial period for the suspended solid samples; however, band F showed increasing signal intensity with operation

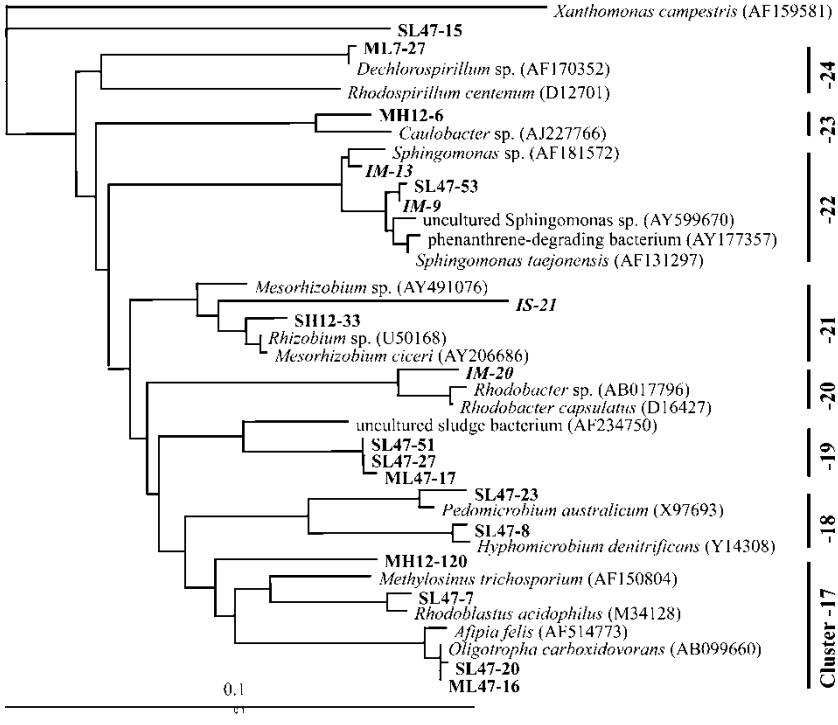

Figure 8. Phylogenetic tree of the *α-Proteobacteria* clones and isolates. Cluster 17 to 24 represent *Bradyrhizobiaceae*, *Hyphomicrobiaceae*, unclassified group, *Rhodobacter*, *Phyllobacteriaceae*, *Sphingomonadaceae*, *Caulobacteraceae* and *Rhodospirillaceae* family or group of the *α-Proteobacteria*, respectively. Other notation is as described for Fig. 5.

time for the membrane samples, indicating that the type of *γ-Proteobacteria* that this band represents changes its growing site, that is, from the suspended solid phase to the membrane surface during operation periods.

Characteristics of Bacterial Isolates from Membrane Surface

Identification of Isolates

Among 20 colonies obtained from sample MH12, only four colonies belonged to *γ-Proteobacteria*, whereas, 15 of 23 colonies obtained from SH12 were assigned to *γ-Proteobacteria* (Table 2). Colonies belonging to the *Bacillus* subclass of *Firmicutes* isolated from both samples MH12 and SH12 were abundant (Table 2). Five colonies isolated from MH12 belonged to *Flavobacteria*, whose phyla were not found in clone libraries. Twenty colonies were

screened and we obtained 11 isolates, and their characteristics as well as sequencing results of representative isolates are shown in Table 4. Most of the isolates were highly identical (>97.0%) to known bacterial species. Several isolates, such as dark-yellow strain IS-21, and deep-yellow strains IM-4, IM-9, and IM-10, had low identities with their closest microorganisms. Most of the membrane isolates were gram-positive, whereas most of the suspended solid isolates were gram-negative.

The isolates were compared with whole clones obtained in this study, particularly with the clones obtained under the low-VOL condition. The phylogenetic tree (Fig. 5) showed that in *γ-Proteobacteria*, isolate IM-17 was similar to clone ML7-9 with 99% similarity, isolate IM-10 was close to both clones ML47-22 and ML7-6 with 99% similarity; in *α-Proteobacteria*, isolate IM-9 showed 99% identity with clone SL47-53. On the other hand, strains that were highly similar to clones, particularly to those groups of the *γ-Proteobacteria* that dominated on the membrane surface under the high-VOL condition, were not isolated by this method.

Characterization of Isolates

Membrane isolates IM-1, 4, 9, 10, 17, 18, and 19, and suspended solid isolates IS-5, 6, 7, 12, 13, 17, and 21, respectively, were selected for characterization of isolates. Because isolates IM-4, IM-10, and IS-21 could hardly grow in the nutrient broth, they could not be characterized in this study.

As Figure 4 shows, the growth curves of the membrane isolates and suspended solid isolates were distinctly different. The suspended solid isolates showed similar patterns of growth curves, and the OD_{600} was near 0.6 to 0.7 after incubation for 10 to 16 h. In contrast, most of the membrane isolates showed unique patterns of growth curves: IM-1 and IM-18 grew faster than the other membrane isolates; IM-17, its OD_{600}, did not increase further after reaching approximately 0.3 to 0.4 after incubation for 30 h; the OD_{600} of IM-19 increased rapidly 0.07 to 0.7 after incubation for 30 h; IM-9 grew slowly. The comparison of growth curves indicated that growth rate of the membrane isolates were distinctly lower than that of the suspended solid isolates.

Cell surface hydrophobicity and EPS concentration were compared among several isolates (Table 5). Before the comparison of hydrophobicity, we confirmed that cell hydrophobicity decreased slightly from the log growth phase to the death phase but did not affect the comparison of different isolates. Except for IM-1, most of membrane isolates showed higher hydrophobicities than the suspended solid isolates. Comparing the EPS concentrations, most of the membrane isolates had higher EPS concentrations in which protein accounts for more than 90% of EPSs. This result was verified further by comparing IS-7 and IM-18; both had similar EPS concentrations.

Table 4. Bacteria isolated from the membrane sample MH12 and the suspended solids sample SH12

Isolate	Color of colony	Closest microorganisms (Accession no.)	Bacterial division	Identity %	Gramm staining
IS-1	White	*Bacillus cereus* (AY138271)	*Firmicutes*	99.8	+
IS-4	White	*Aeromonas hydrophila* (X87271)	*γ-Proteobacteria*	99.9	ND
IS-5	White	*Acinetobacter junii* (AB101444)	*γ-Proteobacteria*	97.5	–
IS-6	Light yellow	*Acinetobacter* sp. (AF430124)	*γ-Proteobacteria*	99.0	–
IS-7	Light yellow	*Aeromonas hydrophila* (X60404)	*γ-Proteobacteria*	99.8	–
IS-12	Light yellow	*Vogesella indigofera* (AB021385)	*β-Proteobacteria*	97.1	–
IS-13	White	*Acinetobacter junii* (AF417863)	*γ-Proteobacteria*	98.1	–
IS-17	White	*Acinetobacter* sp. dcm5A (AF430124)	*γ-Proteobacteria*	99.4	–
IS-20	White	*Acidovorax temperans* (AF078766)	*β-Proteobacteria*	99.7	ND
IS-21	Dark yellow	*Mesorhizobium* sp. (DQ088161)	*α-Proteobacteria*	85.0	+
IS-23	Yellow	*Bacillus subtilis* subsp. (Z99104)	*Firmicutes*	99.9	+
IM-1	White	*Bacillus anthracis* (AY138381)	*Firmicutes*	99.5	+
IM-4	Deep yellow	*Riemerella anatipestifer* (AY871828)	*Flavobacteria*	95.5	+
IM-9	Deep yellow	*Sphingomonas taejonensis* (AF131297)	*α-Proteobacteria*	96.3	+
IM-10	Deep yellow	*Xanthomonas sp.* (DQ011535)	*γ-Proteobacteria*	95.1	+
IM-13	White	*Sphingomonas taejonensis* (AF131297)	*α-Proteobacteria*	98.7	+
IM-14	Yellow	*Ideonella* sp. (AB049107)	*β-Proteobacteria*	97.5	ND
IM-16	White	*Comamonas testosteroni* (M11224)	*β-Proteobacteria*	99.9	ND
IM-17	Yellow	*Pseudomonas alcaligenes* (Z76653)	*γ-Proteobacteria*	99.8	+
IM-18	Yellow	*Pandoraea* sp. (AF247698)	*β-Proteobacteria*	99.7	+
IM-19	Deep yellow	*Arthrobacter rhombi* (Y15885)	*Actinobacteria*	99.8	+
IM-20	Yellow	*Rhodobacter capsulatus* (D16427)	*α-Proteobacteria*	97.3	+

IS-1 to IS-23, bacterial isolates from the suspended solids sample SH12; IM-1 to IM20, bacterial isolates from the membrane sample MH12.

Table 5. Cell surface hydrophobicity and EPS concentration of isolates

		EPS, mg/(mg dry biomass)			
Isolate	Hydrophobicity	TOC	Carbohydrate	Protein	Protein/EPS
IS-7	0.053	0.71	0.16	0.28	0.63
IS-17	0.294	0.54	0.14	0.31	0.69
IM-1	0.060	1.39	0.13	1.21	0.90
IM-9	0.655	2.39	0.19	2.14	0.92
IM-17	0.326	–	–	–	–
IM-18	0.555	0.72	0.05	0.71	0.93
IM-19	0.384	7.56	0.77	6.70	0.90

DISCUSSION

Despite that much effort has been spent, membrane fouling is still a problem hindering the wide spread use of MBR. Considering microbial relevant factors e.g., EPS, soluble microbial products (20) related to membrane fouling, we presume that a microbial approach may provide a novel trigger for controlling membrane fouling. However, a lack of basic information about microbial communities on the membrane surface, particularly in a long-term MBR system that is required for practical processes, averts researchers' attention from the potential. Our study is the first to investigate the structure of bacterial communities on the membrane surface in comparison with those on suspended solids in a submerged MBR treating real wastewater. Our results, obtained by PCR-DGGE and PCR cloning of 16S rDNA genes, showed that the structures of bacterial communities in the suspended solids and on the membrane surface were obviously different, and suggest that *γ-Proteobacteria* more selectively adhere and grow on the membrane surface than other microorganisms.

In practical MBR processes, before TMP increases to 20 kPa higher than initial value (provided by membrane manufacturer, Mitsubishi Rayon), a washing step is necessary to avoid significant membrane fouling. In this study, however, no washing steps were carried out intentionally in order to obtain significantly fouled membranes. Some organisms corresponding to bands A to E existed in the nonsignificantly fouled membranes from the initial stage and did not show any trends with membrane fouling. However, some groups of *γ-Proteobacteria* corresponding to bands F and I, were multiplied with operation time. The comparison between before and after significant fouling of membranes suggest that the bacteria multiplying with operation time are more responsible for membrane fouling than those existing from the initial stage. Because initial-stage of biofilm development has been studied in many model organisms (21, 22), initial-stage observation has been emphasized in studies of membrane fouling (23, 24). Although

microbial communities on the membrane surface can be viewed as a biofilm, they are distinctly different from the usual biofilm because they easily survive on the membrane surface by assimilating nutrients that were supplied by membrane permeation. For this reason together with our results, long-term investigations of the community structure on the membrane surface are very important for identifying fouling-causing bacteria.

Under the low-VOL condition, the organisms associated with the *Xanthomonadacea* family of *γ-Proteobacteria* were predominant on the membrane surface. Considering that many *Xanthomonas* species have been identified as biopolymer-producing biopolymer bacteria (25, 26), this species may play an important role in membrane fouling mechanisms. However, under the high-VOL condition, all organisms suspicious as fouling-causing bacteria were categorized as unidentified *γ-Proteobacteria*. The understanding of the role of these microorganisms for membrane fouling is important. In order to investigate the role, it requires their isolation and characterization. Unfortunately, our isolation procedure could not isolate the target organisms. This result was expected because of those non-culturable or unidentified clone sequences as well as the limitation of culture-dependent method.

Regardless of the phylogenetic distribution, the characteristics of the membrane isolates were clearly different from the suspended solid isolates. Most of the membrane isolates grew slowly as compared with the strains isolated from the suspended solids. Also, the membrane isolates were higher cell surface hydrophobicities, higher EPS concentrations, and higher ratios of protein to carbohydrate within the EPSs than the isolates from suspended solids. These results suggest that among slow-growing bacteria in mixed liquor, those with thick-EPS-layer and high-cell surface hydrophobicity may selectively grow on the membrane surface.

ACKNOWLEDGMENTS

This research was supported by Japan Society for the Promotion of Science under the program of Grants-in-Aid for Scientific Research, Kakenhi, Scientific Research (S) (PI: Kazuo Yamamoto).

REFERENCES

1. Stephenson, T., Judd, S., Jefferson, B., and Brindle, K. (2000) *Membrane Bioreactors for Wastewater Treatment*; IWA Publishing: London.
2. Yamamoto, K., Hiasa, M., Mahmood, T., and Matsuo, T. (1989) Direct solid-liquid separation using hollow fiber membrane in an activated sludge aeration tank. *Wat. Sci. Tech.*, 21: 43–54.
3. Ishida, H., Yamata, Y., Tsuboi, M., and Matsumura, S. (August 30–September 1993). Kubota submerged activated sludge process (KSMAS-P). Its application

into activated sludge process with high concentration of MLSS. Presented at the International Congress on Membranes and Membrane Processes (ICOM'93), Heidelberg.
4. Field, R.W., Wu, D., Howell, J.A., and Gupta, B.B. (1993) Critical flux concept for microfiltration fouling. *J. Memb. Sci.*, 100 (3): 259–272.
5. Cote, P. and Buisson, H. (1997) Immersed membrane activated sludge for the reuse of municipal wastewater. *Desalination*, 113 (2–3): 189–196.
6. Chua, H.C., Arnot, T.C., and Howell, J.A. (2002) Controlling fouling in membrane bioreactors operated with a variable throughput. *Desalination*, 149 (1–3): 225–229.
7. Tomaszewska, M. and Mozia, S. (2002) Removal of organic matter from water by PAC/UF system. *Water Res.*, 36 (16): 4137–4143.
8. Mukai, T., Takimoto, K., Kohno, T., and Okada, M. (2000) Ultrafiltration behaviour of extracellular and metabolic products in activated sludge system with UF separation process. *Water Res.*, 34 (3): 902–908.
9. Hodgson, P.H., Leslie, G.L., Schneider, R.P., Fane, A.G., Fell, C.J.D., and Marshall, K.C. (1993) Cake resistance and solute rejection in bacterial microfiltration: the role of the extracellular matrix. *J. Membr. Sci.*, 79: 35–53.
10. Leslie, G.L., Schneider, R., Fane, A.G., Marshall, K.C., and Fell, C.J.D. (1993) Fouling of a microfiltration membrane by two gram-negative bacteria. *Colloids and Surfaces A: Physicochemical and Engineering Aspects.* 73: 165–178.
11. Luxmy, B.S. (2000) Analysis of Microbial Communities and their Interrelationship in the Membrane Separation Activated Sludge Process. PhD thesis, Department of Urban.
12. Witzig, R., Manz, W., Rosenberger, S., Krüger, U., Kraume, M., and Szewzyk, U. (2002) Microbiological aspects of a bioreator with submerged membranes for aerobic treatment of municipal wastewater. *Water Res.*, 36 (2): 394–402.
13. Muyzer, G., Waal, E.C., and Uitterlinden, A.G. (1993) Profiling of complex microbial populations by denaturing gradient gel electrophoresis analysis of polymerase chain reaction-amplified genes coding for 16S rRNA. *Appl. Environ. Microbiol.*, 59: 695–700.
14. Lane, D.J. (1991) 16S/23S rRNA sequecing. In *Nucleic Acid Techniques in Bacterial Systematics*. Stackebrandt, E. and Goodfellow, M. (eds.), Wiley & Sons: Chichester, United Kingdom, 115–175.
15. Altschul, S.F., Gish, W., Miller, W., Myers, E.W., and Lipman, D.J. (1990) Basic local alignment search tool. *J. Mol. Biol.*, 215 (3): 403–410.
16. Thompson, J.D., Higgins, D.G., and Gibson, T.J. (1994) CLUSTAL W: improving the sensitivity of progressive multiple sequence alignment through sequence weighting, position-specific gap penalties and weight matrix choice. *Nucleic Acids Res.*, 22 (22): 4673–4680.
17. Saitou, N. and Nei, M. (1987) The neighbor-joining method: a new method for reconstructing phylogenetic trees. *Mol. Biol. Evol.*, 4 (4): 406–425.
18. Dubois, M., Gilles, K.A., Hamilton, J.K., Rebers, P.A., and Smith, F. (1956) Colorimetric method for determination of sugars and related substances. *Anal. Chem.*, 28: 350–356.
19. Rosenberg, M., Gutnick, D., and Rosenberg, E. (1980) Adherence of bacteria to hydrocarbons: a simple method for measuring cell-surface hydrophobicity. *FEMS Microbial Letters*, 9: 29–33.
20. Duncan, J. Barker and David, C. Stuckey. A review of soluble microbial products (SMP) in wastewater treatment systems. *Wat. Res.*, 33 (14): 3063–3082.

21. Chandra, J., Kuhn, D.M., Mukherkee, P.K., Hoyer, L.L., Cormick, T.Mc., and Ghannoum, M. (2001) Biofilm formation by the fungal pathogen Candida albicans: development, architecture, and drug resistance. *J. Bacteriol.*, 183: 5385–5394.
22. Loo, C.Y., Corliss, D.A., and Ganeshkumar, N. (2000) Streptococcus gordonii biofilm formation: identification of genes that code for biofilm phenotypes. *J. Bacteriol.*, 182: 1374–1382.
23. Wendong, Xu. and Shankararaman, Chellam (2005) Initial stages of bacterial fouling during dead-end microfiltration. *Environ. Sci. Technol.*, 39: 6470–6476.
24. Zhang, Kai., Choi, H., Dionysios, D. Dionysios, George, A. Sorial., and Daniel, B. Oerther (2006) Identifying pioneer bacterial species responsible for biofouling membrane bioreactors. *Environ. Microbiol.*, 8 (3): 433–440.
25. Moreira, A.S., Vendruscolo, J.L.S., Gil-Turnes, C., and Vendruscolo, C.T. (2001) Screeing among 18 novel strains of *Xanthomonas campestris* pv pruni. *Food Hydrocolloids*, 15 (4–6): 469–474.
26. Benjamin, P. Kemp, Jennifer, Horne, Alan, Bryant, and Richard, M. Cooper (2004) Xanthomonas axonopodis pv. manihoris gumD gene is essential for EPS production and pathogenicity and enhances epiphytic survival on cassava (Manihot esculenta). *Physiological and Molecular Plant Pathology*, 64: 209–218.